

28p.

NASA
Technical Memorandum 83765

USAAVSCOM
Technical Report 84-C-13

Response of a Small-Turboshaft-Engine Compression System to Inlet Temperature Distortion

(NASA-TM-83765) RESPONSE OF A
SMALL-TURBOSHAFT-ENGINE COMPRESSION SYSTEM
TO INLET TEMPERATURE DISTORTION (NASA) 28 p
CSCL 21E

N87-10100

Unclas
G3/07 44355

Thomas J. Biesiadny
*Lewis Research Center
Cleveland, Ohio*

Gary A. Klann
Propulsion Laboratory
AVSCOM Research and Technology Laboratories
*Lewis Research Center
Cleveland, Ohio*

and

Jeffery K. Little
*Lewis Research Center
Cleveland, Ohio*

Date for general release September 1986

September 1984



RESPONSE OF A SMALL-TURBOSHAFT-ENGINE COMPRESSION
SYSTEM TO INLET TEMPERATURE DISTORTION

Thomas J. Biesiadny
National Aeronautics and Space Administration
Lewis Research Center
Cleveland, Ohio 44135

Gary A. Klann
Propulsion Laboratory
AVSCOM Research and Technology Laboratories
Lewis Research Center
Cleveland, Ohio 44135

Jeffery K. Little
National Aeronautics and Space Administration
Lewis Research Center
Cleveland, Ohio 44135

SUMMARY

E-2198

An experimental investigation was conducted into the response of a small-turboshaft-engine compression system to steady-state and transient inlet temperature distortions. Transient temperature ramps ranged from less than 100 deg K/sec to above 610 deg K/sec and generated instantaneous temperatures to 420 K above ambient. Steady-state temperature distortion levels were limited by the engine hardware temperature limit. Simple analysis of the steady-state distortion data indicated that a particle separator at the engine inlet permitted higher levels of temperature distortion before onset of compressor surge than would be expected without the separator.

INTRODUCTION

An experimental investigation was conducted in a ground-level test facility to determine the response of the compression system of a small turboshaft engine to steady-state and transient temperature distortion. When rotary-wing aircraft hover near the ground, engine exhaust can be contained within the rotor downwash and recirculated to the engine inlet (fig. 1). This reduces both the power available (refs. 1 to 3) and the compression system surge margin (refs. 1 and 3). This effect is similar to gun or rocket exhaust gas ingestion. The confident prediction of reingestion levels for any arbitrary helicopter/engine design and their effect on engine performance requires a comprehensive set of design data not currently available (refs. 3 and 4). Typically, model and flight tests have been conducted to measure the magnitude and effects of this ingestion (ref. 3). Although the total problem of hot gas ingestion is complex and involves many factors, temperature distortion is probably the principal factor affecting the performance and stability limits of the engine.

The research reported herein is one step toward a better understanding of the response of a typical small turboshaft engine to hot gas ingestion in the

controlled environment of a ground-level test facility. A temperature distortion device, consisting of a gaseous hydrogen burner with individually controlled 45° sectors, was installed upstream of an engine inlet to produce steady-state and transient temperature distortion patterns. The engine was instrumented with steady-state and high-response probes to record engine inlet conditions and engine response. The transient temperature ramps ranged from less than 100 deg K/sec to above 610 deg K/sec and generated instantaneous temperatures to 420 K above ambient. Surge and nonsurge conditions were produced as the engine operated at and above the maximum power setting for continuous engine operation. The steady-state temperature distortion level was kept below the engine inlet hardware limits. The temperature transient results presented include typical engine response in terms of pressures and temperatures; temperature rise versus temperature rise rate for 45°, 90°, and 180° extent circumferential distortions; and a comparison of test results with those from flight tests.

APPARATUS

Engine

The engine (fig. 2) used for the investigation was a front-drive, turbo-shaft engine comprising an integral particle separator; a single-spool gas generator section consisting of a five-stage axial-flow, single-stage centrifugal-flow compressor, a throughflow annular combustor, and a two-stage, axial-flow gas generator turbine; and a free two-stage, axial-flow power turbine.

Instrumentation

The instrument station locations and the distribution of instrumentation at each station are shown in figure 3 (see appendix A for symbols). The engine compression system was heavily instrumented with high-response and steady-state pressure instrumentation to record its response to inlet temperature distortion. Because the compressor inlet (station 2) was surrounded by hardware, instrument station locations were limited to two borescope ports. Even the station 2 instrumentation that was available was not used for these tests because of the overpressure during surge. The same was true of the instrumentation at station 2.5. The absence of instrumentation at station 2 prevented a direct determination of the effect of the inlet particle separator on the temperature distortion entering the engine.

Test Facility

The engine was tested by using Jet A fuel in a ground-level test facility that has an atmospheric inlet and atmospheric as well as altitude exhaust capability (fig. 4). The hardware required to support the testing included an eddy-current dynamometer rated at 1640 kW, a gearbox with 3.743:1 gear ratio, an inlet bellmouth, an airflow measurement spool piece, a temperature distortion generator, and a device to measure airflow dumped overboard through a scavenge blower on the engine.

Temperature Distortion Generator

The temperature distortion generator could create both steady-state and time-variant, or transient, temperature distortion at the engine inlet by using gaseous hydrogen. It was an adaptation of a device described in reference 5. The burner (fig. 5) consisted of eight individually controlled sectors, with three swirl cup combustors (fig. 6) per sector. Not shown are stainless steel straps between the cups in each sector, which aided flame propagation. Many sector combinations or temperature distortion patterns were possible. The hydrogen distribution system from the fuel supply point to the swirl cup combustors and its operation are described in detail in reference 6.

PROCEDURE

Temperature Distortion

In a typical operation to find the response of the engine to inlet temperature distortion, the burner was lit while the engine was at idle. The hydrogen flow was adjusted in those sectors where the temperature distortion was being imposed, and the engine was brought up to the desired operating condition. Once conditions were stabilized, the hydrogen flow was either increased to a fixed level to produce the desired steady-state distortion or, if a transient distortion was desired, pulsed at increasingly greater pressures until stall occurred. Each pressure pulse produced a unique combination of temperature rise and temperature rise rate at the engine inlet. If surge occurred, the hydrogen flow was stopped and the engine was brought to a lower operating speed either manually by the engine operator or automatically by the facility detection system.

Thermocouple Correction Factors

The thermocouple-indicated temperature was corrected for time lag as follows:

$$T_{act} = T_{ind} + \tau (\Delta T/\Delta t)_{ind}$$

The time constant values τ calculated for the engine inlet temperature probes are displayed in table I. The time constants for the probe were measured and then averaged from three runs performed over each of six Mach number conditions. Within each three-run set, the measured time constants showed close agreement. The calibration procedure is described further in appendix B.

RESULTS AND DISCUSSION

The results of an experimental investigation to determine the response of a small turboshaft engine, particularly the compression system, to steady-state and transient inlet temperature distortions are presented. These results include typical compression system response in terms of compressor operating point, pressures, and temperatures; the effect of circumferential distortion extent; and a comparison of the results produced in the ground-level test facility to those obtained in flight.

Steady-State Distortion

Attempts were made to measure the magnitude of the steady-state distortion required to surge the engine. None of these attempts were successful because the distortion levels that could be imposed were limited by the engine inlet hardware temperature limit of 395 K. However, a simplified analysis of the compressor operating point during these steady-state distortion tests indicated that the particle separator desensitized the engine to the extent of circumferential temperature distortion possibly by redistributing and mixing the heated and unheated inlet air to produce a more uniform temperature profile at the compressor face.

By way of explanation see figure 7, a plot of the uniform-inlet-flow compressor map generated experimentally by injecting air at the centrifugal compressor discharge. Plotted on the compressor map is a steady-state data point where a 180° circumferential temperature distortion was created at the engine inlet (solid triangle). The engine did not surge for these conditions up to the steady-state temperature limit for the engine inlet hardware. Assuming that the compressor inlet will see the 180° circumferential distortion imposed at the engine inlet, the average compressor operating point will be on the operating line, as shown by the solid triangular symbol. This represents the compressor speed corrected to sea-level static (SLS) conditions by using the average engine inlet temperature, 323 K. From parallel compressor theory assumptions (ref. 7), the two sectors of the compressor will operate at the same pressure ratio but different corrected speeds, as indicated by the solid diamond symbol for the hot sector (i.e., the compressor speed corrected to SLS conditions by using only the average hot (distorted) inlet temperature, 350 K) and the solid cone symbol for the cold sector (i.e., the compressor speed corrected to SLS conditions by using only the average cold (undistorted) inlet temperature, 295 K). As shown, the hot sector operating point crossed the compression system surge line and should have caused the compressor to surge. Since no surge occurred, the compressor inlet probably did not see a pure 180° distortion but saw a more homogeneous flow possibly caused by mixing in the particle separator.

Time-Dependent Distortion

A typical inlet temperature rise produced by the temperature distortion generator that produced surge and the response of selected compression system pressure transducers are shown in figure 8. The compression system itself could tolerate the transient temperature distortion up to a certain combination of temperature rise and rise rate until the onset of surge. As shown in figure 8, the surge was evident from the engine inlet, station 1, to the compression system discharge, station 3.

Instantaneous time history traces of high-response pressure transducers at selected stations from the engine inlet to the compression system discharge are shown in figure 9. The dominant feature of these figures is the 22-Hz surge, of approximately 0.4-sec duration, that persisted from compressor inlet to discharge. During this time there was also evidence at each of the compressor stations of a pressure falloff that increased with each stage.

The compressor system response shown in figure 9 was typical of that encountered during all of the transient temperature distortion testing whether

45°, 90°, or 180° circumferential extent distortion was present. Because the 1/2 sec or less time for the duration of the surge was similar to that encountered in the field (ref. 2), there is some degree of confidence that these types of temperature transient simulate the effect of hot gas ingestion in flight.

Transient Circumferential Distortion Extent

A simplified analysis indicated that if the inlet temperature was increased, the corrected compressor speed would decrease. If this temperature rise was faster than the rate of decrease in the compressor pressure ratio, the compressor operating point would approach the surge line. If only part of the inlet annulus was heated, the unheated area would help maintain the compressor pressure ratio. The result was a lower temperature rise rate required for surge than if the whole annulus was heated.

The steady-state data showed an apparent influence of the inlet particle separator on the compression system's tolerance to inlet temperature distortion. The transient data were examined for evidence of this effect. From inlet temperature distortion work on turbine engines (ref. 7) it could be postulated that, as the circumferential extent increased from 45° to 180°, compressor surge would be more likely to occur. The data presented herein show this to be true. However, because the inlet particle separator tended to homogenize the inlet flow, the temperature levels reached before surge occurred were much higher than those for turbojet engines without inlet particle separators.

It is also of interest to compare the adjacent and nonadjacent zones of distortion encountered for two and four 45° extent distortions. For nonadjacent zones the engine was less likely to surge than for adjacent zones when the same number of zones were distorted. It can be postulated that for the nonadjacent zones the inlet particle separator presented a more balanced flow pattern at the compressor face. Thus the compressor was better able to tolerate the distortion. A secondary consideration is that if the engine inlet temperature sensor saw the temperature and caused the corrected speed to be driven low enough, the start bleed valve would have opened and given the compressor additional surge margin.

A more detailed presentation of the transient data results for 45°, 90°, and 180° distortion with an extrapolation to a full face, or 360°, distortion follows.

45° extent. - The results of inlet temperature distortion transients in one sector (45°) of the hydrogen burner at a time are shown in figure 10. This plot of temperature rise against temperature rise rate shows that the highest temperatures and greatest temperature rise rates were attained in the zone, zone 4, facing the sensor that measured inlet temperature and whose signal was sent to the engine hydromechanical unit for variable-geometry adjustments (i.e., of the inlet guide vanes, compressor stators, and start bleed valve). The temperature signal was used to adjust the inlet guide vanes and compressor stators toward more cambered positions in order to allow a larger surge margin at a given speed.

In zones in which the inlet temperature sensor was not present, a temperature rise of 310 K and a rise rate of 339 deg K/sec were reached without surge occurring. With the inlet temperature sensor present, the temperature rose 404 K and the rise rate was 460 deg K/sec, at least a 30 percent improvement over the results in the other zones. The simplified analysis previously presented suggested that, without an inlet particle separator, the temperature rise to produce surge would have been approximately 220 deg K.

90° extent. - Because of the versatility of the hydrogen burner, circumferential distortions of 90° extent, or two zones, could be created either with adjacent zones (one 90° extent or "1 per rev") or nonadjacent zones (two 45° extents or "2 per rev"). The results of such an investigation are shown in figure 11 for two nonadjacent zones and in figure 12 for two adjacent zones. The closer the two distortion zones, the less tolerant to the transient temperature distortion, or more prone to surge, was the compression system (fig. 11). For instance, with zones 1 and 7 distorted, a temperature rise of only 195 K and a ramp rate less than 228 deg K/sec were possible without surge occurring. In contrast, when zones 3 and 7 were distorted, a temperature rise about 85 deg K higher and a ramp rate more than double were possible.

A two-zone combination that included the zone facing the inlet temperature sensor, zone 4, was more tolerant than the combinations where it was excluded. A temperature rise of 390 K and a rise rate of approximately 610 deg K/sec were possible before the onset of surge. The findings presented in figure 11 with regard to the relationship between the proximity of two distorted zones and the likelihood of compressor surge were reinforced by the results presented in figure 12, where the two zones are adjacent. Excluding the combination using zone 4, the maximum attainable temperature rise and rise rate before surge were approximately 208 K and 222 deg K/sec. These values are close to those shown in figure 11 for zones 1 and 7 in combination. Again, making zone 4 part of the distortion pattern allowed a higher temperature rise and a higher rise rate before surge.

When the zone where the inlet temperature sensor saw the temperature distortion was excluded, the compression system had a lower temperature rise and a lower rise rate before surge for a distortion extent of two zones than for one zone. Compare the results in figure 10 with those in figures 11 and 12.

180° extent. - The results of three four-zone, or 180° extent, transient temperature distortion patterns are shown in figure 13. In two cases the four zones were adjacent, but one combination included the zone with the inlet temperature sensor whereas the other excluded it. In the third case the zones were nonadjacent and excluded zone 4. As in the distortion patterns of 45° and 90° extent, when the inlet temperature sensor saw the temperature distortion, it did allow for some variable-geometry adjustments. The results for the adjacent distorted zones were a temperature rise of approximately 178 K and a rise rate of 179 deg K/sec as compared with a rise of approximately 172 K and a rise rate of approximately 167 deg K/sec when the sensor did not see the distortion. Granted the differences were not as large as with the 45° and 90° extents, but still they were detectable. As for the 45° and 90° distortions the compression system was less tolerant for the 180° extents than for the 90° extent. Also, when the zones were nonadjacent, surge was delayed longer (i.e., temperature rise and rise rate were higher) than when the zones were adjacent.

360° extent. - A full-face, or 360° extent, distortion was not investigated because higher than normal engine oil temperatures were encountered while all eight zones of the hydrogen burner were being set up and balanced before the temperature transients were taken. The results shown in figure 14, however, may give some indication as to what might have occurred had this type of distortion been possible. This figure summarizes the temperature rise possible before the onset of surge with various circumferential distortion extents. These data exclude the results where zone 4 was distorted. The trend in this figure is toward a leveling off of temperature rise with increasing extent as 180° is reached. Similar results were seen in an investigation involving steady-state temperature distortion (ref. 8), where it was noted that between 90° and 180° extent there was not a significantly large change in compression system response.

An extrapolation of the results shown in figure 14 to a full-face or 360° extent distortion was attempted. In the field a temperature rise of approximately 77 deg K was recorded (ref. 2) just before surge. This is close to the value that would be obtained from an extrapolation of figure 14 data assuming that the field engine saw a full-face temperature distortion. Note that many more thermocouples were used in the test facility to document the inlet conditions than was possible in flight (ref. 2).

Power Level Influence

Inlet temperature distortion transients were limited to engine operation at the maximum power setting for continuous engine operation, or maximum continuous power, in order to minimize the chance of a turbine overtemperature during surge. An exception to the power restriction was a single operation at intermediate rated power (IRP), or the maximum power setting of a 30-min duration, to investigate the effect of power level on the results presented in figures 10 to 13. The data at maximum continuous power and intermediate rated power for a 180° extent distortion are shown in figure 15. The engine power setting was inversely proportional to the maximum temperature rise and maximum temperature rise rate reached before onset of surge. As power was increased from maximum continuous to IRP, the temperature rise decreased approximately 11 K and the temperature rise rate decreased over 28 deg K/sec at the onset of surge.

CONCLUDING REMARKS

An experimental investigation was undertaken to determine the response of a small turboshaft engine compression system to steady-state and transient inlet temperature distortions. It was determined that engine response in the test facility environment was similar to that in the field with regard to the duration of the surge. The maximum temperature rises to produce surge appeared to be similar although the test facility data required an extrapolation, which increased the uncertainty of those results. Generally, the temperature distortion generator can be used to simulate the principal factor involved in hot gas ingestion encountered in the field, temperature distortion, with some degree of confidence that the results are applicable.

Additional findings were the following:

1. The steady-state data showed that the inlet particle separator desensitized the effect of the circumferential temperature distortion at the compressor face.

2. For 45°, 90°, and 180° extents, the greater the extent during inlet temperature transients, the more likely was the engine compression system to surge.

3. The engine compression system was slightly more tolerant to temperature distortion transients if the engine inlet temperature sensor saw the hot gas. This was possible because the engine control could make variable-geometry adjustments.

4. For nonadjacent zones of transient temperature distortion, the greater the distance between the zones, the more tolerant was the engine compression system to distortion.

5. The inlet particle separator's tendency to mix the flow before it reached the compressor face apparently permitted the compressor to reach much higher steady-state and transient temperature levels before onset of surge than would be expected if no particle separator were present.

6. From the small amount of data taken at other than maximum continuous power it appears that as power level increased the maximum temperature rise and rise rate reached before onset of surge decreased.

APPENDIX A
SYMBOLS

M	stream Mach number
P	total pressure, kPa
P _s	static pressure, kPa
T	temperature, K
T _i	initial temperature, K
T ₀	final temperature, K
t	time, sec
θ	circumferential extent, deg
τ	thermocouple time constant, sec
τ ₀	reference time constant, sec

Subscripts:

act	actual
ind	indicated
0.5	station 0.5, airflow measuring station
1	station 1, engine inlet
1.3	station 1.3, scavenge blower discharge
2	station 2, axial compressor stages
2C-2M	station 2C-2M, axial compressor stages
2.5	station 2.5, axial compressor discharge
3	station 3, centrifugal compressor discharge
4.5	station 4.5, gas generator turbine exit and power turbine inlet
7	station 7, exhaust duct inlet

APPENDIX B

CALIBRATION OF A THERMOCOUPLE PROBE USED FOR TURBOSHAFT ENGINE TESTS

This appendix briefly describes the calibration of a Chromel-Alumel thermocouple probe used during the turboshaft engine tests. The purpose is to acquaint others with a general thermocouple calibration procedure and also to present specific time-constant data for a certain thermocouple probe. A schematic view of the probe is presented in figure 16.

The calibration consisted of acquiring the necessary data to calculate the time constant τ for the Chromel-Alumel thermocouple. The time constant of a system is usually defined as the time required for the system to reach 63.2 percent of its steady-state value (ref. 9). The value of 63.2 percent comes from the fact that many time-varying functions can be represented by the exponential relation

$$T = (T_1 - T_0)e^{-t/\tau} + T_0 \quad (1)$$

When $t = \tau$, equation (1) becomes

$$T = (T_1 - T_0)e^{-1} + T_0 = 0.368 (T_1 - T_0) + T_0 \quad (2)$$

In other words, when $t = \tau$, the difference between T and T_1 is 63.2 percent of the difference between the initial and steady-state values of T . This situation is displayed in figure 17.

The procedure used to obtain the time constant of the probe in this investigation is quite simple. The experimental setup is shown in figure 18 (a modification of a figure from ref. 10). The probe, mounted to receive flow from a nozzle, was heated to an initial excited state by a hot-air blower. While being heated, the thermocouple was protected from the ambient conditions of the nozzle flow by a simple shield. Once the thermocouple achieved equilibrium in the excited state, the shield and the hot-air source were pneumatically removed at the same instant, and the thermocouple was exposed to the air flowing from the nozzle.

The response of the excited thermocouple to the nozzle flow was recorded on both a digital voltmeter and a strip-chart recorder. The voltmeter readings were necessary to calibrate the strip chart. In an example strip-chart recording shown in figure 19 (from ref. 11) the time constant of the probe τ was measured as the recorded time required to reach $0.368 (T_1 - T_0)$ on the temperature scale.

The value of τ_0 will vary with respect to various nozzle flow conditions and initial thermocouple temperatures. Reference 10 suggests using the expression

$$\tau_0 \approx \tau \sqrt{\frac{MP_s}{101.325}} \left(\frac{T_{ind}}{555} \right)^{0.18} \quad (3)$$

to calculate a reference time constant τ_0 . This time constant should remain a constant for a particular probe over a wide range of flow and initial temperature conditions.

The time constant values calculated for the probe (fig. 16) are displayed in table I. The time constants for the probe were measured and then averaged from three runs performed over each of six Mach number conditions. Within each three-run set the measured time constants showed very close agreement. Between the sets the time constants increased as expected with each decrease in flow Mach number. Apparently, the reference time constant equation becomes invalid for stream Mach numbers of 0.10 or less, but a fairly steady value of τ_0 was found over the Mach number range 0.15 to 0.40. This value could possibly remain constant beyond Mach 0.40, but the calibration was based on expected flow conditions in the engine tests that did not exceed Mach 0.40.

REFERENCES

1. Sheridan, P. F.; and Wiesner, W.: Aerodynamics of Helicopter Flight Near the Ground. AHS Paper 77-33-04, 1977.
2. Turczeniuk, Bohdan: Exhaust Gas Reingestion Measurements. AHS Paper HPS-23, 1979.
3. Jackson, M. E.; and House, R. L.: Exhaust Gas Reingestion During Hover In-Ground-Effect. Proceedings, American Helicopter Society, 37th Annual Forum, New Orleans, La., May 17-20, 1981, pp. 378-385.
4. NASA Advanced Rotorcraft Technology Task Force Report. 1978, p. VIII-12.
5. Pawlik, E. V.; and Jones, R. E.: Experimental Evaluation of Swirl-Can Elements for Propane-Fuel Combustor. NASA Memo 5-15-59E, 1959.
6. Klann, Gary A.; Barth, Richard; and Biesiadny, Thomas J.: Temperature Distortion Generator for Turbohaft Engine Testing. NASA TM-83748, 1984.
7. Graber, E. J.; and Braithwaite, W. M.: Summary of Recent Investigations of Inlet Flow Distortion Effect on Engine Stability. NASA TM X-71505, 1974.
8. Mehalic, C. M.; and Lottig, R. A.: Steady-State Inlet Temperature Distortion Effects on the Stall Limits of a J85-GE-13 Turbojet Engine. NASA TM X-2990, 1974.
9. Holman, Jack P.; and Gajda, W. J.: Experimental Methods for Engineers. McGraw-Hill, Inc., 1978, p. 25.
10. Glawe, G. E.; Holanda, R.; and Krause, L. N.: Recovery and Radiation Corrections and Time Constants of Several Sizes of Shielded and Unshielded Thermocouple Probes for Measuring Gas Temperature. NASA TP-1099, 1979.
11. Scadron, Marvin D.; and Warshawsky, Isidore: Experimental Determination of Time Constants and Nusselt Numbers for Bare-Wire Thermocouples in High-Velocity Air Streams and Analytic Approximation of Conduction and Radiation Errors. NASA TN-2599, 1952.

TABLE I. - TIME CONSTANT CALIBRATION RESULTS

[Stream total pressure, P, 99.35 kPa.]

Stream Mach number, M	Probe indicated temperature, T_{ind} , K	Thermocouple time constant, τ , sec	Thermocouple reference time constant, τ_0 , sec
0.40	344	0.222	0.12
.30	337	.253	.12
.20	342	.300	.12
.15	344	.365	.12
.10	342	.490	.14
0	350	1.05	0

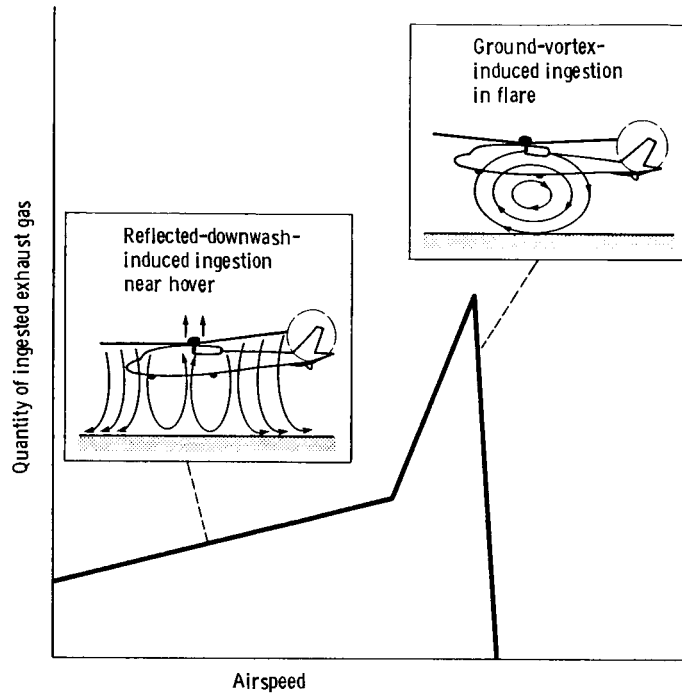


Figure 1. - Patterns of exhaust ingestions near ground. (From ref. 1.)

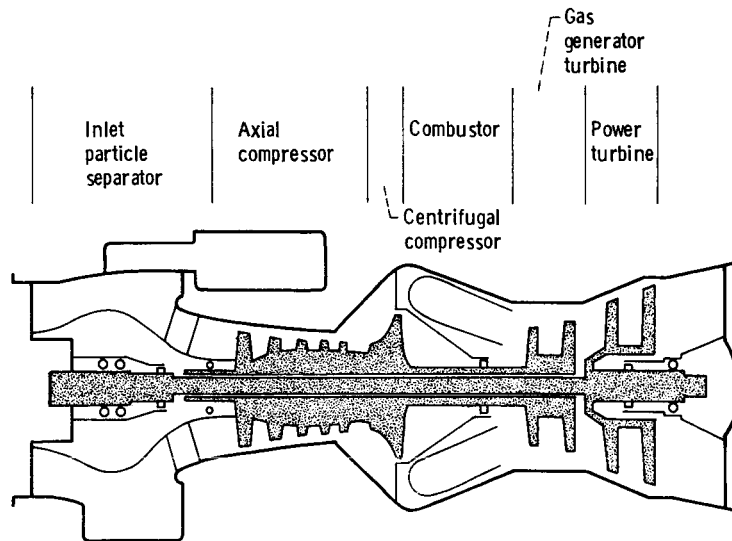
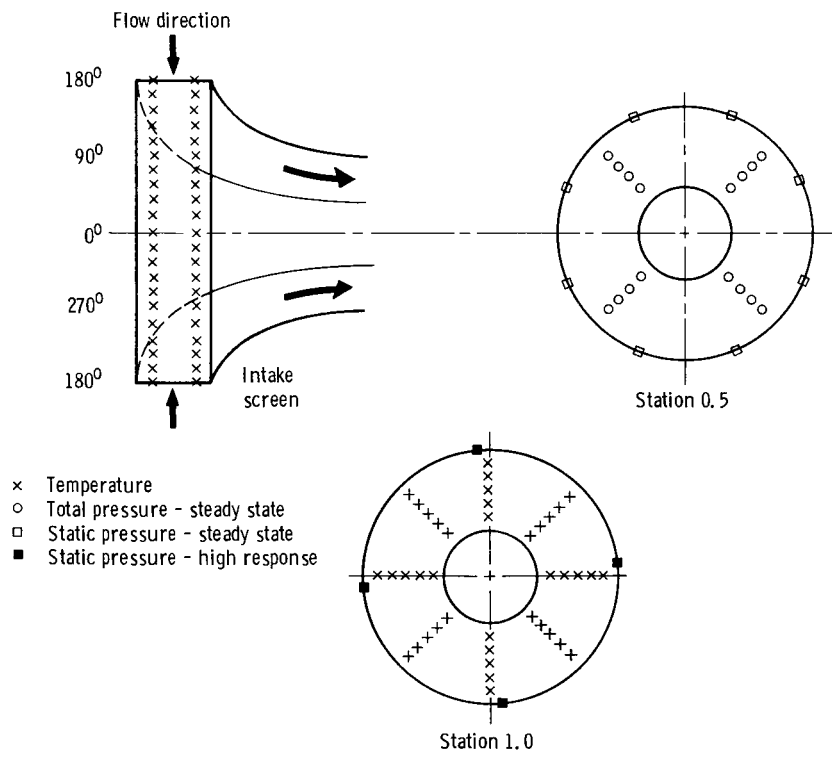
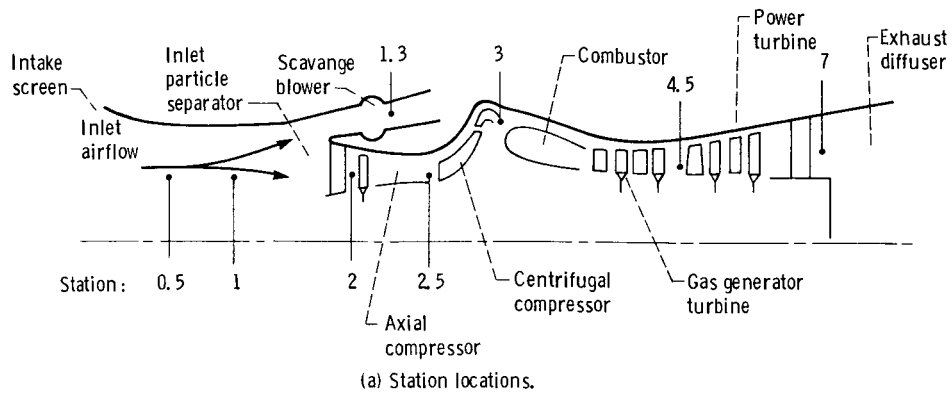
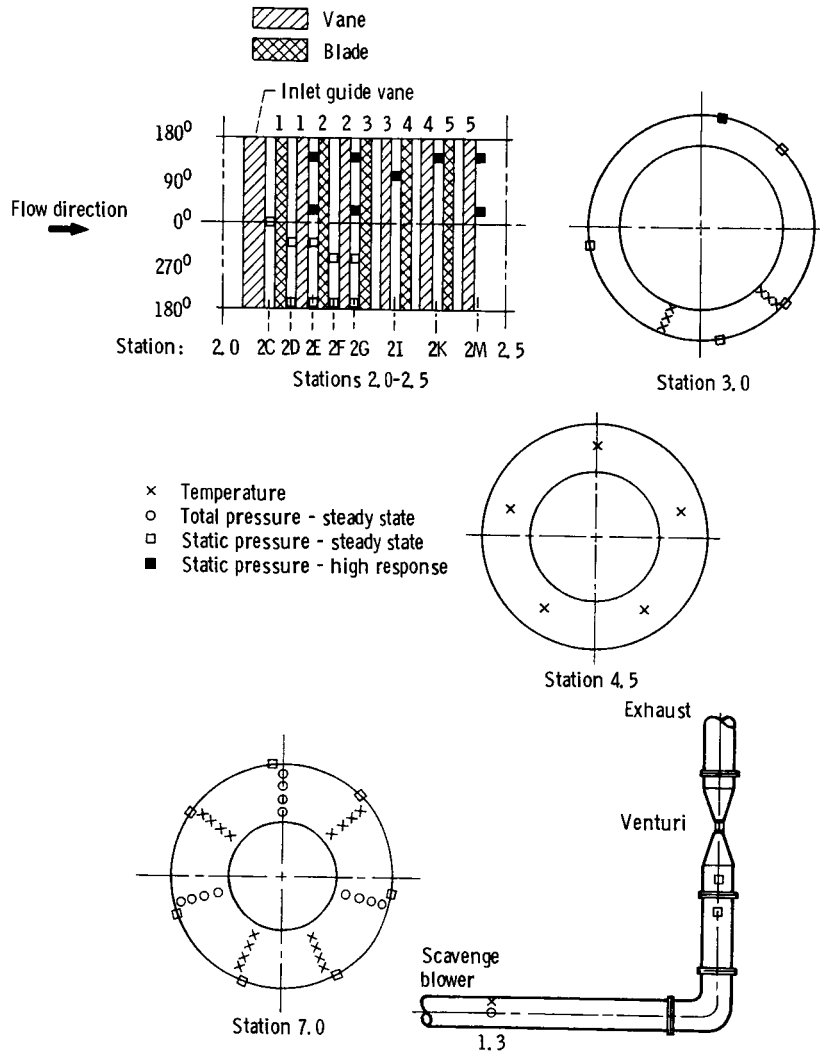


Figure 2. - Schematic of engine.



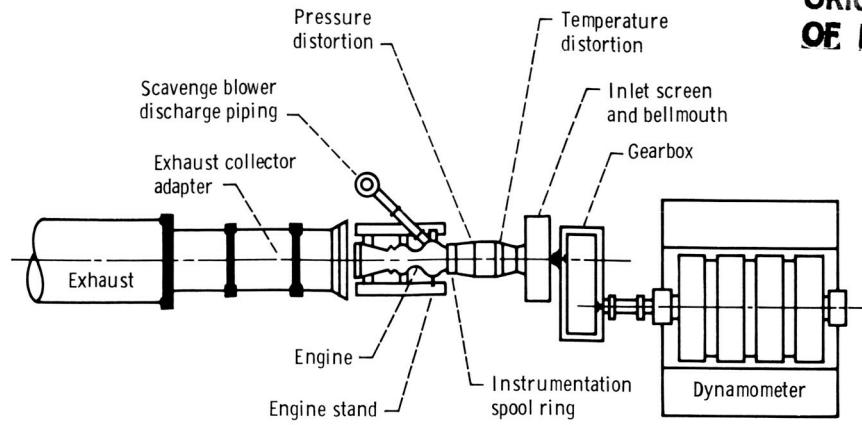
(b) Station layout. Aft - looking forward.
 Figure 3. - Instrumentation locations.



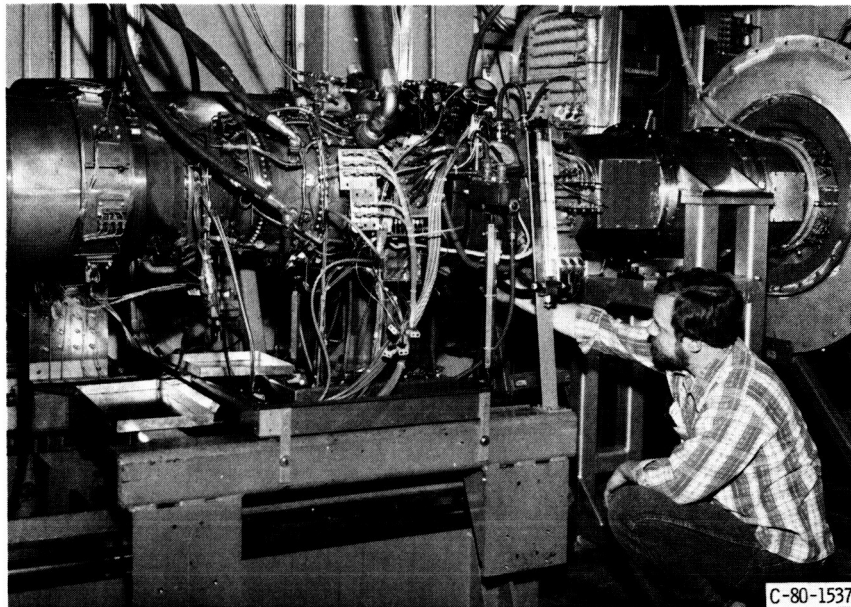
(b) Concluded.

Figure 3. - Concluded.

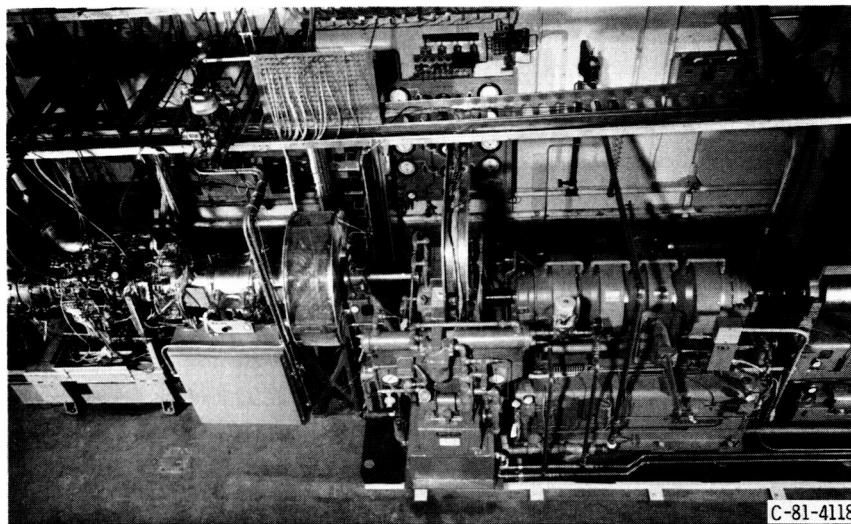
ORIGINAL PAGE IS
OF POOR QUALITY



(a) Plan view (not to scale).



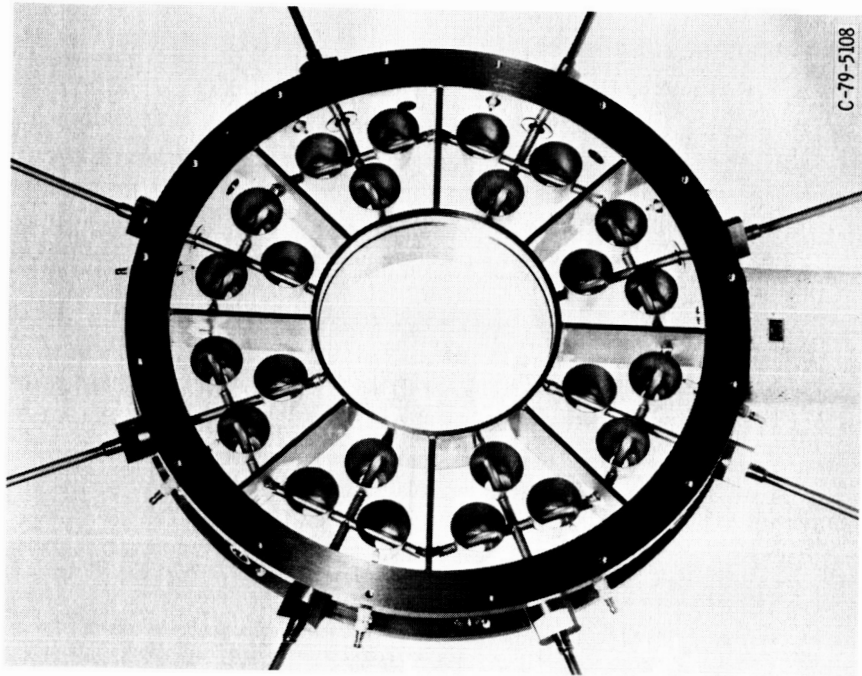
(b) Engine installation.



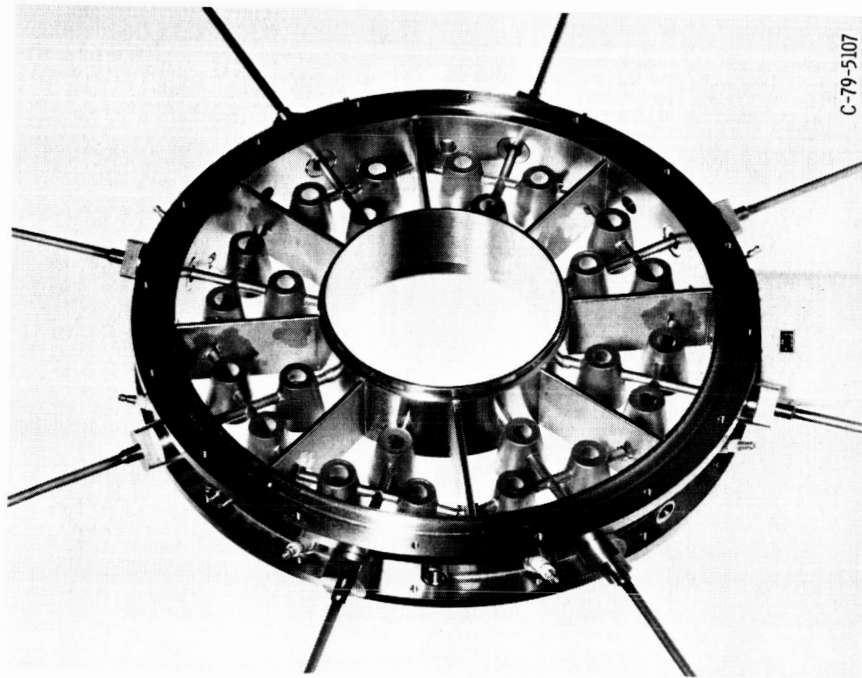
(c) Test cell overview.

Figure 4. - Test cell.

ORIGINAL PAGE IS
OF POOR QUALITY



(b) Looking upstream.



(a) Looking downstream.

Figure 5. - Temperature distortion generator.

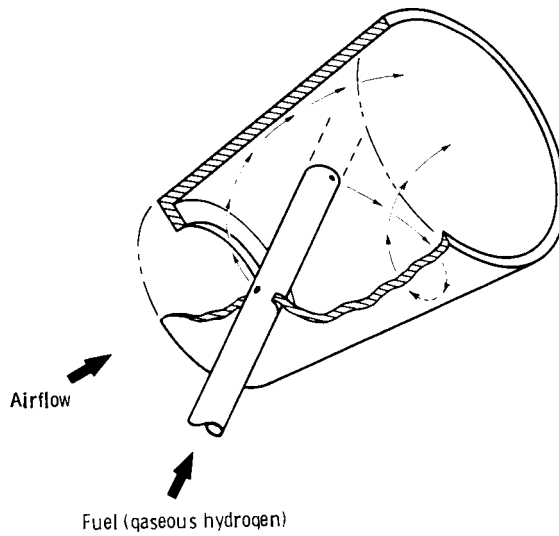


Figure 6. - Operation of typical swirl-cup combustor.

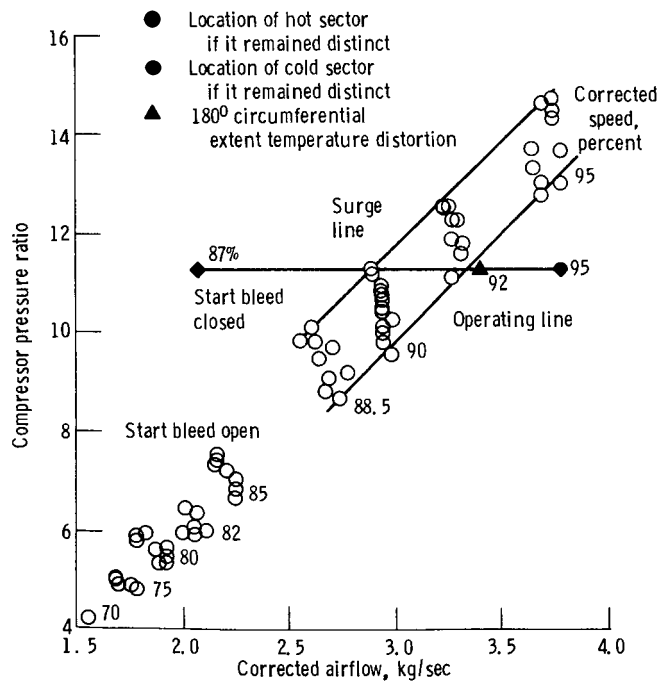


Figure 7. - Typical compressor performance map, showing effects of mixed and unmixed distorted areas.

ORIGINAL PAGE IS
OF POOR QUALITY

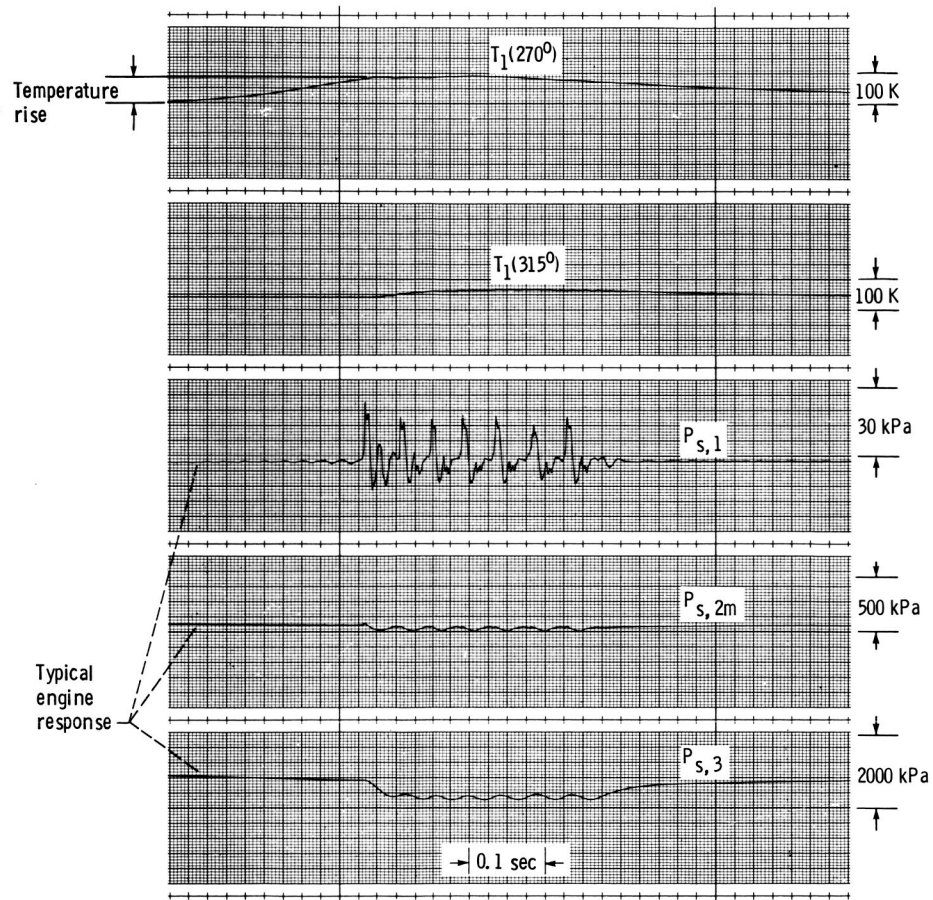


Figure 8. - Typical response to a transient inlet temperature distortion.

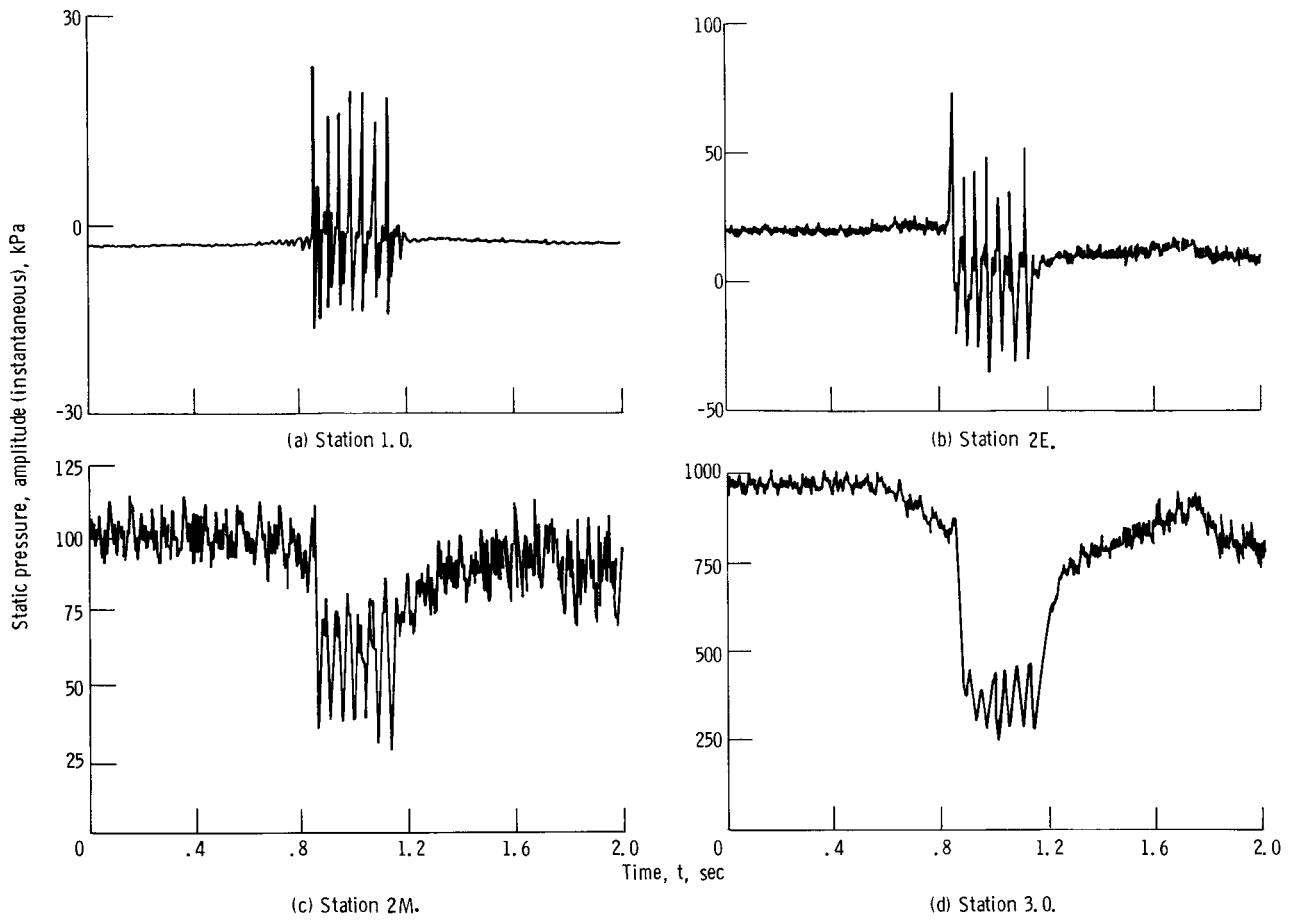


Figure 9. - Instantaneous time history of compressor response.

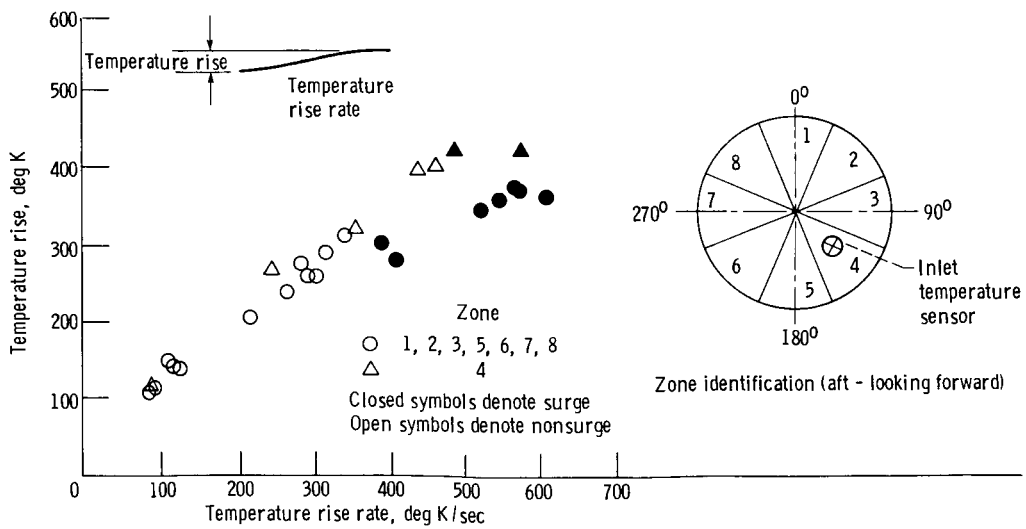


Figure 10. - Transient inlet temperature distortion - 45° extent.

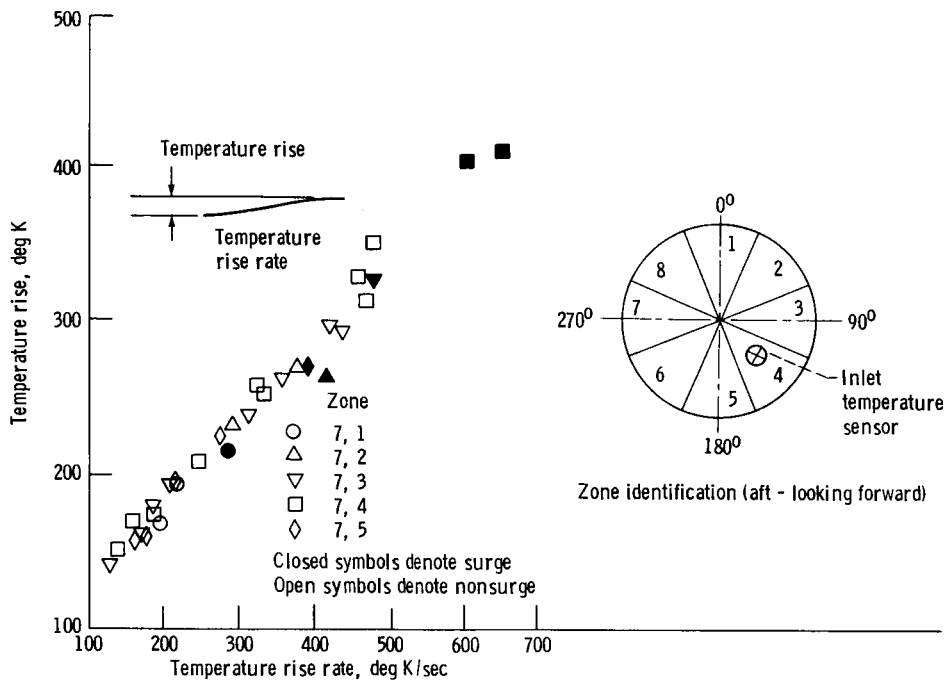


Figure 11. - Transient inlet temperature distortion - two nonadjacent 45° extents.

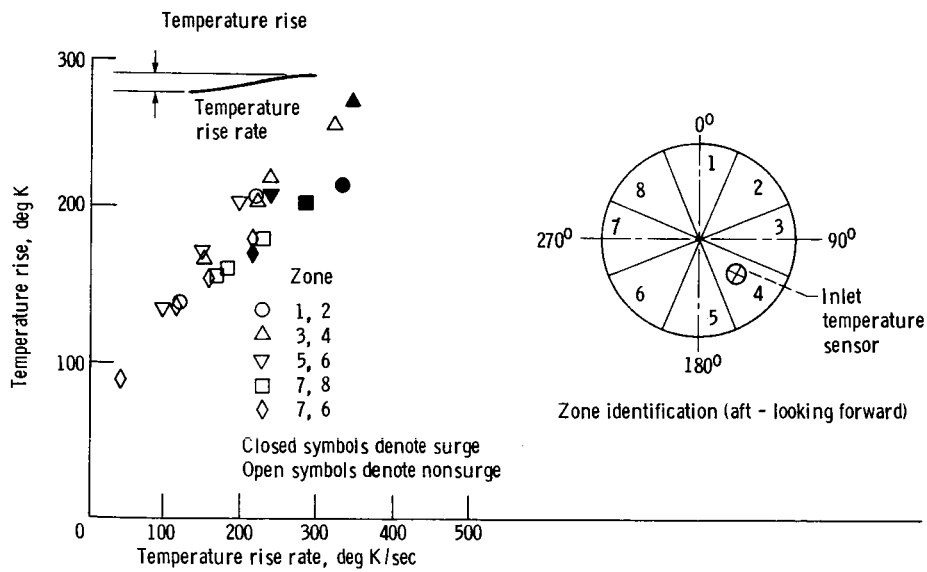


Figure 12. - Transient inlet temperature distortion - two adjacent 45° extents.

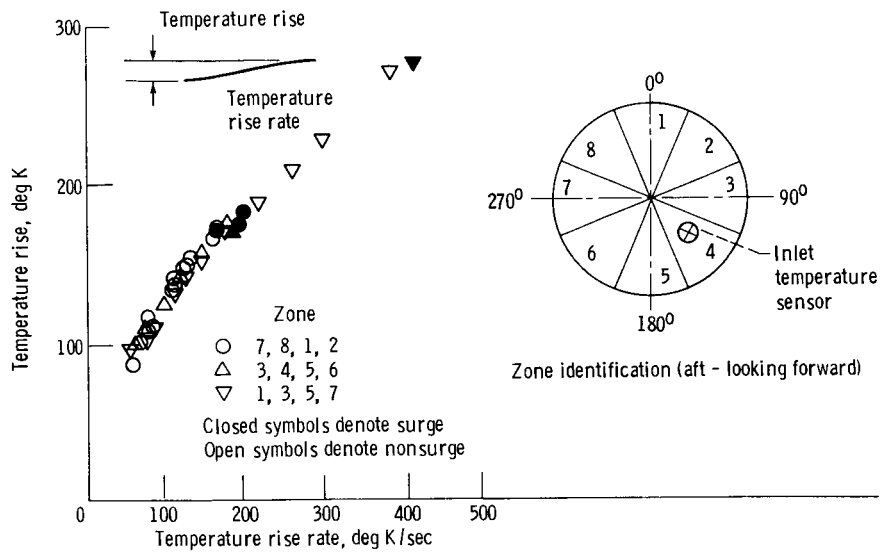


Figure 13. - Transient inlet temperature distortion - four 45° extents, adjacent and non-adjacent.

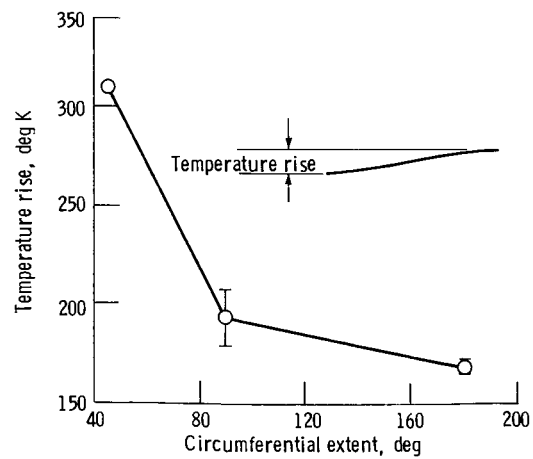


Figure 14. - Inlet temperature rise before onset of surge as a function of circumferential extent, zone 4 excluded.

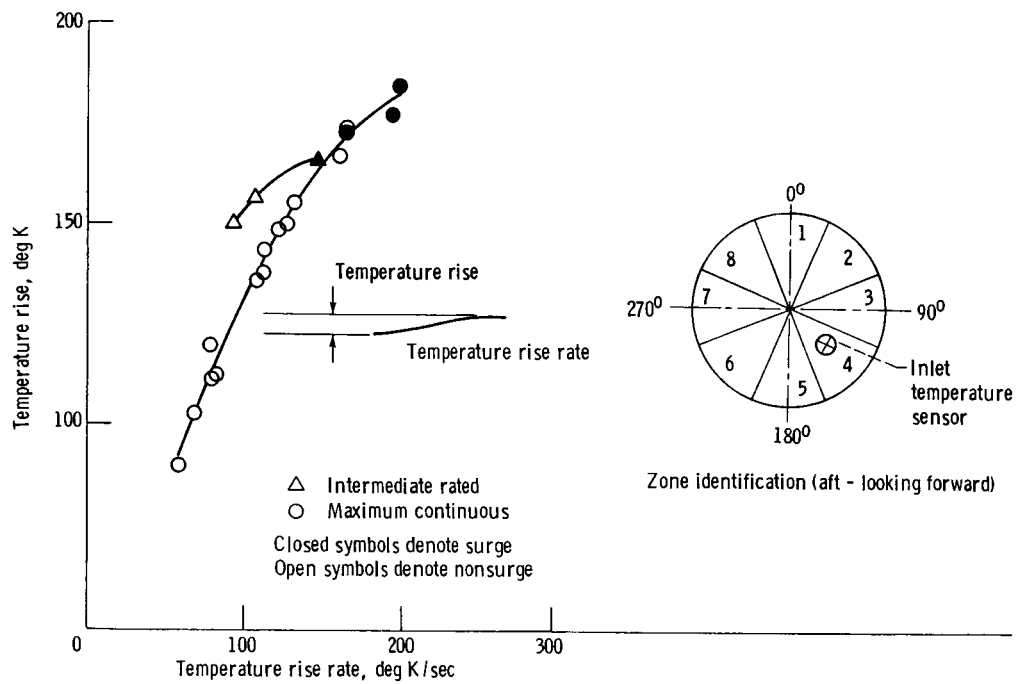


Figure 15. - Variation of transient inlet temperature distortion with power setting - zones 7, 8, 1, and 2.

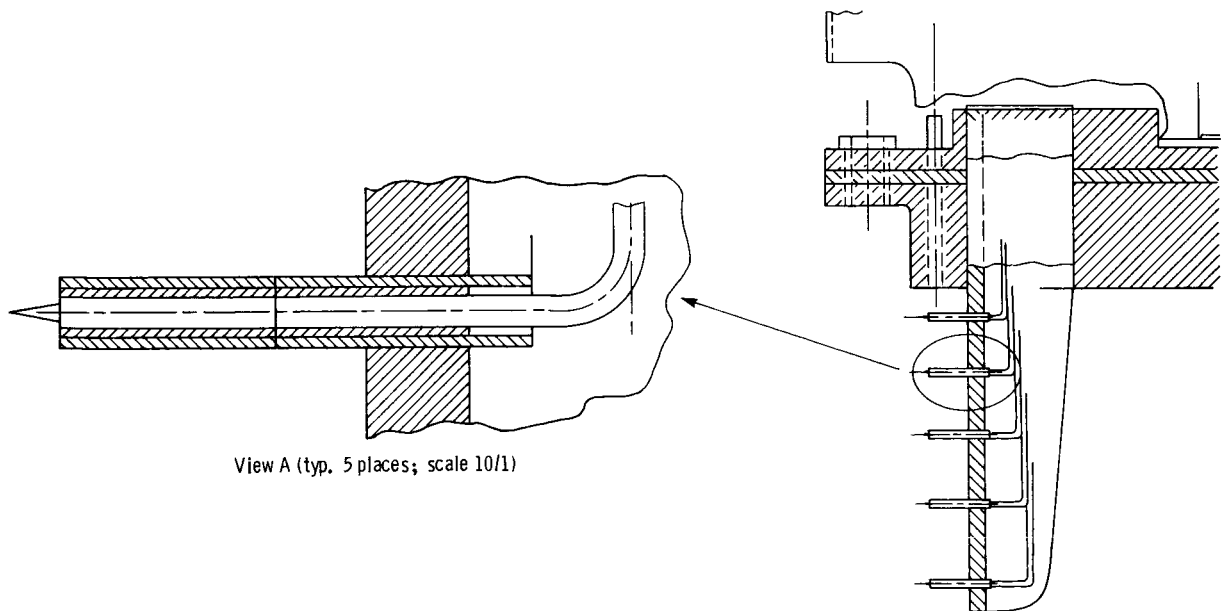


Figure 16. - Chromel-Alumel thermocouple probe.

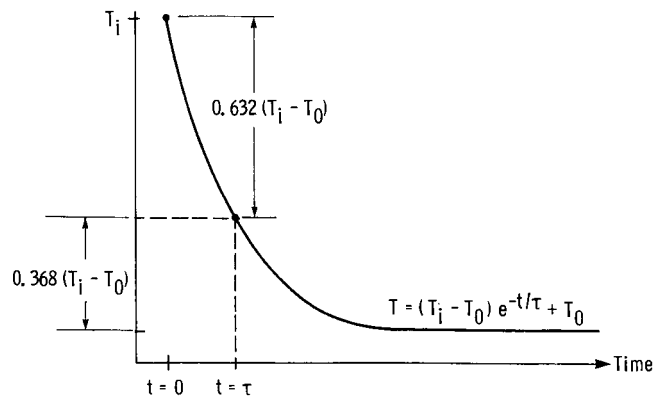


Figure 17. - Exponential decay curve.

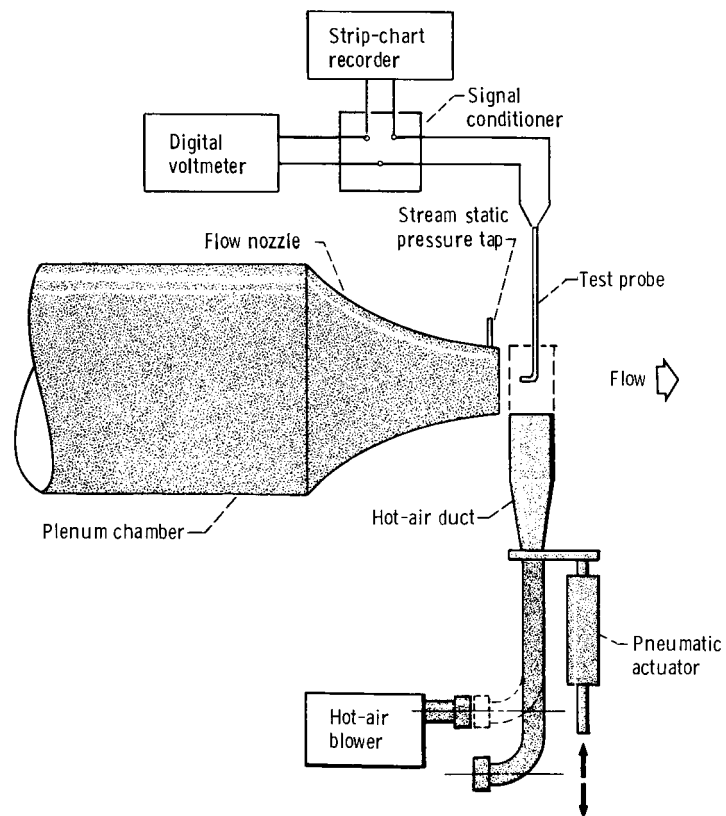


Figure 18. - Time-constant test apparatus. (Adapted from ref. 10.)

ORIGINAL PAGE IS
OF POOR QUALITY

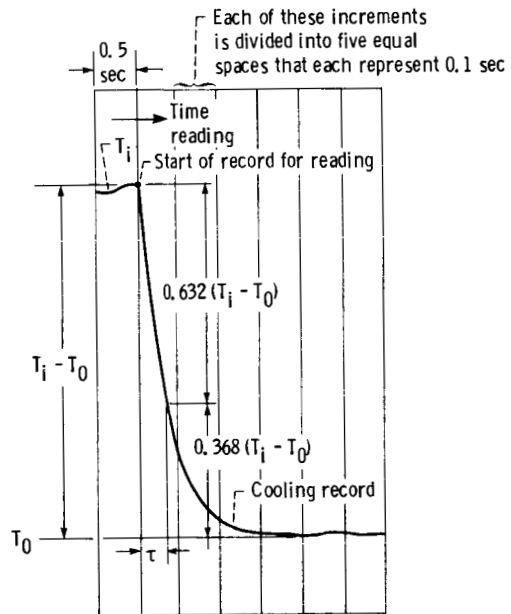


Figure 19. - Sample record. (From ref. 11.)

1. Report No. NASA TM-83765 USAAVSCOM-TR-84-C-13		2. Government Accession No.		3. Recipient's Catalog No.	
4. Title and Subtitle Response of a Small-Turboshaft-Engine Compression System to Inlet Temperature Distortion				5. Report Date September 1984	
				6. Performing Organization Code 505-32-6A	
7. Author(s) Thomas J. Biesiadny, Gary A. Klann, and Jeffery K. Little				8. Performing Organization Report No. E-2198	
				10. Work Unit No.	
9. Performing Organization Name and Address NASA Lewis Research Center and Propulsion Laboratory U.S. Army Research and Technology Laboratories (AVSCOM) Cleveland, Ohio 44135				11. Contract or Grant No.	
				13. Type of Report and Period Covered Technical Memorandum	
12. Sponsoring Agency Name and Address National Aeronautics and Space Administration Washington, D.C. 20546 and U.S. Army Aviation Systems Command, St. Louis, Mo. 63120				14. Sponsoring Agency Code	
15. Supplementary Notes Thomas J. Biesiadny, NASA Lewis Research Center; Gary A. Klann, Propulsion Laboratory, AVSCOM Research and Technology Laboratories, Lewis Research Center, Cleveland, Ohio 44135; Jeffery K. Little, NASA Lewis Research Center.					
16. Abstract An experimental investigation was conducted into the response of a small-turbo-shaft-engine compression system to steady-state and transient inlet temperature distortions. Transient temperature ramps ranged from less than 100 deg K/sec to above 610 deg K/sec and generated instantaneous temperatures to 420 K above ambient. Steady-state temperature distortion levels were limited by the engine hardware temperature limit. Simple analysis of the steady-state distortion data indicated that a particle separator at the engine inlet permitted higher levels of temperature distortion before onset of compressor surge than would be expected without the separator.					
17. Key Words (Suggested by Author(s)) Engine tests Inlet temperature Distortion Surges Turboshafts			18. Distribution Statement Unclassified - [REDACTED] Category 07 [REDACTED]		
19. Security Classif. (of this report) Unclassified		20. Security Classif. (of this page) Unclassified		21. No. of pages	22. Price*